EFSUMB Course Book, 3rd Edition

Editor: Christoph F. Dietrich

Transcranial sonography of brain parenchyma in adults

Uwe Walter[1]

[1]Department of Neurology, Rostock University Medical Center, Rostock, Germany

Corresponding author

Uwe Walter MD, PhD, FEAN

Rostock University Medical Center, Department of Neurology, Rostock, Germany

D-18147 Rostock, Gehlsheimer Str. 20.

uwe.walter@med.uni-rostock.de

On behalf of the European Society of Neurosonology and Cerebral Hemodynamics

Introduction

Transcranial B-mode sonography (TCS) of the brain in adults has been established as a tool for i) the diagnosis and follow-up of neurodegenerative disorders, and ii) the monitoring of midline shift, evolving hydrocephalus and intracranial hemorrhage in neuro-intensive care medicine (1-3). Compared to MRI and computed tomography, TCS has the advantage of high mobility, non-invasiveness, and more robustness against movement artifacts (1, 3, 4). TCS can detect abnormalities of deep brain structures that are not, or only with high effort, visualized with other imaging modalities (5). TCS may guide the insertion of brain electrodes or catheters in real-time. This chapter covers the basic method and clinically relevant applications of TCS.

Examination technique

Equipment and system settings

Advanced TCS applications (e.g. the exact localization of deep brain stimulation electrodes) require the use of a high-end ultrasound system. Some standard applications (e.g., assessment of substantia nigra, measurement of ventricle widths) may be performed with an adequately equipped portable ultrasound system. A phased-array probe with a center frequency of 2.0- to 3.0-MHz (usually 2.5 MHz) is used. The same probes can be chosen as used for transcranial color-coded sonography (TCCS) of intracranial vessels. ‘Matrix’ probes with a higher crystal (channel) density may allow for improved B-mode image resolution. System settings recommended for TCS of brain parenchyma are: dynamic range, 40-60 dB (for ventricle widths: 20-45 dB); post-processing function set at moderate suppression of low echogenic signals; time gain compensation and image brightness to be adapted manually as needed or, if available, by applying automated image optimization (i.e. pressing the referring button on the keyboard, standard with high-end ultrasound systems). Image resolution of 2.5-MHz probes is highest at an image depth of 5-9 cm which is the focal zone of transducer (1, 5). The image resolution in axial direction (i.e. along the axis of ultrasound propagation) is higher than in lateral direction (usually 0.7 × 2 mm; up to 0.7 × 1.1 mm) which is the cause also of some typical imaging artifacts (e.g. the enlargement of small, highly echogenic structures in lateral direction). Distinct measurements, e.g. of echogenic areas of small deep brain structures, are

influenced by chosen system settings as well as by manufacturer-specific image post-processing technology. That is why normal ranges for echogenic area of relevant structures, especially substantia nigra (SN), need to be obtained for each different ultrasound system / system preset and, because of some investigator dependency, advisably for each different lab.

Positioning and maneuvers for the exam

The patient is placed in supine or semi-supine position on an examination chair layer. The investigator sits behind the patient's head. The investigation room should be darkened. Transtemporal TCS is preferred since cranial bone is thinnest at this anatomic region, and relevant brain structures can be visualized. At start, the ultrasound transducer is placed on the right temple near to the ear and parallel to the orbitomeatal line in order to obtain a standardized axial view of intracranial structures [Figure 1A-C]. To control and stabilize the transducer position, the small finger/ulnar edge of the working hand should be continuously in contact with both, the transducer and the patient's head. To find the optimum bone window for insonation, the transducer is moved near (or above) the anterior helix of the ear conch, searching for the position with best visualization of brain and contralateral skull bone.

Tip 1 **Start with imaging depth of 14-16 cm to overview ipsi- and contralateral brain.**

Tip 2 **Utilize pressure, tilting and sliding of the probe to optimize visualization.**

Tip 3 **Scan the diagnostically relevant deep brain structures from both sides.**

Figure 1 **Standard TCS imaging planes for assessment of patients with movement disorders. C = cerebellum, I = insula, M = midbrain, P = pineal gland, T = thalamus, V = lateral ventricle. A) Transducer position for axial transections. B) TCS image of axial transection at thalamus level. C) TCS image of axial transection at midbrain level. D) Transducer position for coronal and semi-coronal**

transections. E) TCS image of coronal transection through thalami. F) TCS image of semi-coronal transection through thalami and midbrain.

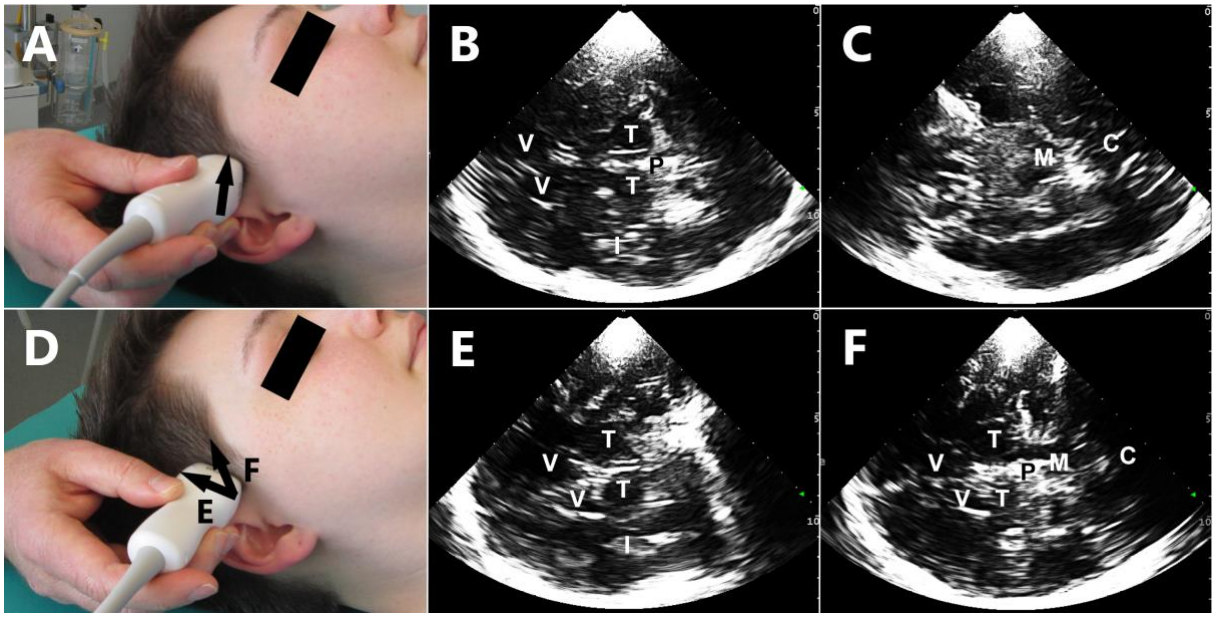

Intracranial landmark structures

Beside the bony structures of the skull, several brain structures can serve as anatomical landmarks for orientation. The visibility of landmark structures depends on the quality of the bone window used for insonation. Partial or complete insufficiency of the transtemporal bone windows is found in 5-40 % of patients depending on age, sex and geographic origin [Figure 2] (4, 5).

Figure 2 **Grades of TCS image quality depending on transtemporal bone window. A) High-quality TCS image with wide display of brain structures and contralateral cortex/skull. B) Moderate-quality TCS image with narrowed display of brain structures. Usually midbrain structures such as substantia nigra can well be assessed. C) Low-quality TCS image with visibility only of echogenic central**

structures such as pineal gland and third ventricle. D) No visibility of brain structures due to thickness and/or osteoporosis of temporal bone.

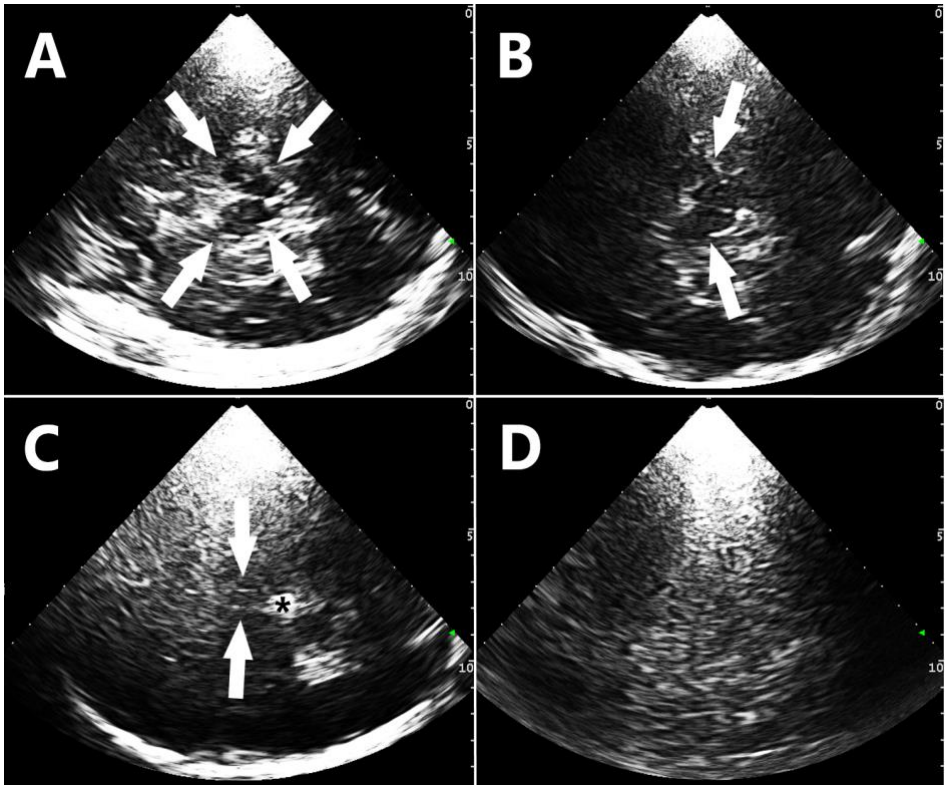

Remember 1 **The TCS image is of good quality if the contralateral skull bone is clearly visualized over its whole extension in the imaging sector.**

Landmarks that can regularly be visualized even in moderate sonographic conditions with identification rates of >75% are mesencephalon with its surrounding basal cisterns [Figure 3], pons, third ventricle, falx, thalamus, pineal gland [Figure 4], parts of lateral ventricles and temporal lobe. Identification of medulla oblongata, fourth ventricle, cerebellar structures, hippocampus, insula, frontal, parietal and occipital lobes is more difficult.

Figure 3 **Structures assessed at midbrain level in patients with movement or affective disorders. A) TCS image of axial transection at midbrain level. The butterfly-**

shaped midbrain surrounded by basal cisterns (arrows) is clearly displayed. B) Zoom of TCS image shown in (A) with clearly visible echo signals of substantia nigra (arrow head), red nucleus (arrow), raphe and aqueduct (*).

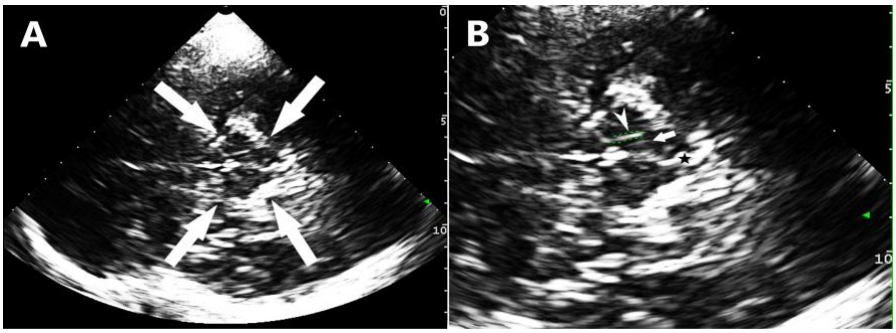

Figure 4 **Structures assessed at thalamus level in movement and other brain disorders. C = caudate head, F = frontal horn of lateral ventricle, I = insula, L = lenticular nucleus, P = pineal gland, Pl = choroid plexus of dorsal horn of lateral ventricle, T = thalamus. A) TCS image of axial transection at thalamus level. Note that lenticular and caudate nucleus cannot be distinguished by their echogenicity from the surrounding brain parenchyma. B) Zoom of TCS image shown in (A) with measuring marks (crosses) placed in the inner edge of the highly echogenic borders of third ventricle (arrows) and frontal horn. The anatomic areas of lenticular and caudate nucleus contralateral to insonation are traced for better recognizability.**

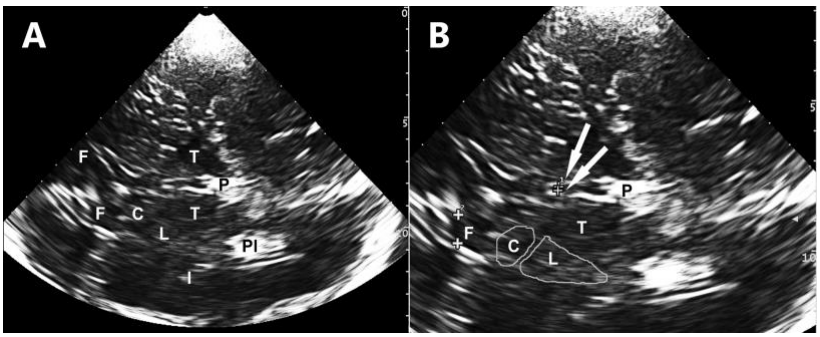

TCS in neurodegenerative disorders

In neurodegenerative diseases transtemporal TCS is usually carried out in standard axial imaging planes [Figures 3, 4]. For some diagnostic questions TCS is additionally performed in semi-coronal and coronal scanning planes, e.g. for assessment of the posterior fossa, or the localization of deep brain stimulation (DBS) electrodes [Figures 1D-E, 5].

Figure 5 **Assessment of deep brain stimulation (DBS) electrodes on TCS. A) MRI-TCS fusion image of coronal transection showing the longitude of DBS electrode ipsilateral to insonation (arrow: tip of electrode visualized on TCS). B) TCS image of coronal transection corresponding to (A). The distal metal pol of the electrode (arrow: tip of electrode) causes reverberation artefacts (triangles) that are to be discriminated from substantia nigra echo signals (arrow head). The close display of electrode tip and the lateral portion of substantia nigra echo signals indicates optimum electrode location in the subthalamic nucleus. C) Axial TCS image corresponding to (B): transection of electrode tip (arrow) is displayed with slight distortion due to ultrasound characteristics (arrow head: substantia nigra echo).**

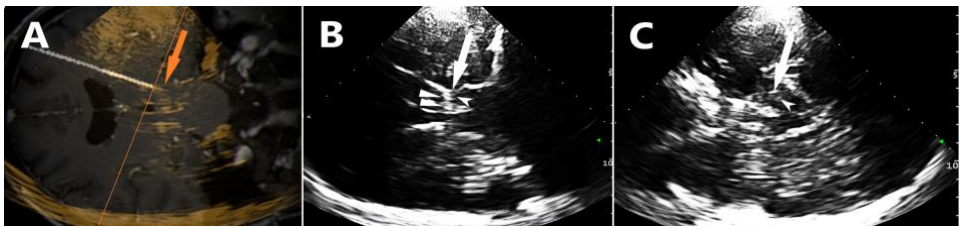

Midbrain plane

Midbrain structures that can be assessed with respect to their echogenicity are SN, raphe, and red nucleus. SN TCS is of highest clinical relevance since it is well established for the early and differential diagnosis of Parkinson's disease (PD) (2, 6). It is useful also for the position control of DBS electrodes in the subthalamic nucleus in patients with PD (7).

Remember 2 **The midbrain us adequately visualized if the butterfly-shaped midbrain transection surrounded by the highly echogenic basal cisterns (cisterna ambiens, cisterna quadrigemina, cisterna suprasellaris) is completely displayed.**

The SN echo signals may have a patchy, a band-like or sometimes a wide oval appearance [Figure 6].

Figure 6 **Inter-individual variation of substantia nigra (SN) echogenicity and its planimetric measurement (individual area tracing shown in the inlet of the referring panel). A) Low echogenicity ('hypoechogenicity') of SN (area measure: 0.05 cm²), often seen in restless-legs syndrome. B) Patchy appearance of normal SN echogenicity (0.12 cm²). Note the typical aspect of brainstem raphe which is displayed as a continuous, highly echogenic line. C) Band-like appearance of normal SN echogenicity (0.13 cm²). D) Moderate SN hyperechogenicity (0.25 cm²). Remember that the, here highly echoic, red nucleus (arrow) should not be included in the tracing of SN echoes. Note the reduced echogenicity of brainstem raphe which is an-echogenic in this case. E) Patchy appearance of marked SN hyperechogenicity (0.35 cm²). F) Band-like appearance of marked SN hyperechogenicity (0.42 cm²), often seen in Parkinson's disease.**

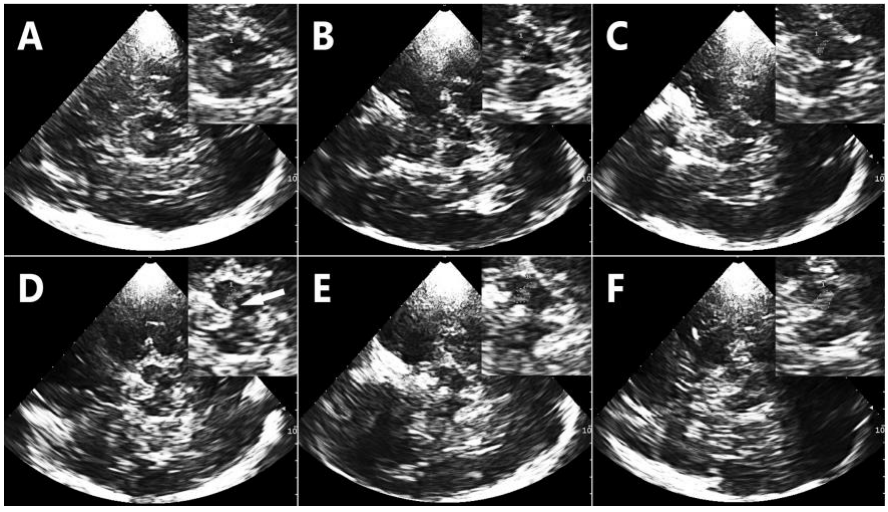

The appearance of SN may slightly vary even in the same individual if using different transducer angulations, or various ultrasound systems (8). The grade of SN echogenicity is usually assessed by planimetric measurement of SN's echogenic signals (SN echogenic area) in axial plane (8, 9). SN echogenic area is, as a standard, measured ipsilateral to insonation in order to avoid interference with reverberation artifacts originating from structures of the basal cisterns. Therefore TCS of right SN is performed from right side, and TCS of left SN from left side. The axial midbrain transection showing the echo signals of ipsilateral SN in its largest extension is identified by slight tilting of the probe. If the representative SN echo signals are seen very clearly the image is frozen immediately. After moving back to the optimum frame using the cine mode if necessary, the midbrain is zoomed out two- to threefold. The SN echogenic signals are surrounded manually by the cursor using the trackball, resulting in automatic calculation of echogenic area. One should avoid the erroneous inclusion of highly echogenic signals of structures neighboring the SN, i.e. red nucleus and basal cisterns (1, 8).

Remember 3 **SN echo signals are adequately visualized if displayed at typical anatomic location in the crus mesencephali and well separated from the echo signals of nucleus ruber and basal cisterns.**

The inter-individual variation of SN echogenicity has been suggested to be caused by a variable degree of local iron accumulation and abnormal iron-protein-compounds but also by gliotic changes (2, 10). Between the 18th and 75th year of age the distribution of SN echogenicity in normal population can be regarded as nearly constant, with a slight increase during adult life decades, which pronounces only at ages >80 years (11-14). To rate SN echogenicity in an individual as normal or increased ("hyperechogenic") the 75% and 90% percentile of measures in normal population are used as a reference, and the larger of bilaterally measured SN echogenic sizes is used for classification as follows: normal echogenic SN present if area measure is below the 75% percentile; moderately hyperechogenic SN present if area measure is between the 75% and the 90% percentile; markedly hyperechogenic SN present if area measure is above the 90% percentile (1). To establish normal ranges for a specific ultrasound

system, at least 50 healthy individuals should be investigated bilaterally to obtain at least 100 measures (2). Otherwise, cut-off values published for various ultrasound systems may be used, which have been summarized earlier (15). In principle SN echogenic area measures <0.20 cm² can be regarded as normal independent from the ultrasound system used, and measures >0.30 cm² are markedly hyperechogenic. The grading of measures in-between 0.20 and 0.30 cm² depends on the specific cut-off values for the ultrasound system and system settings used. It is advisable that investigators starting with ultrasound assessment of SN echogenicity are supervised by an experienced investigator, or take part in a certified ultrasound hands-on course, e.g. of the European Society of Neurosonology and Cerebral Hemodynamics (ESNCH).

SN hyperechogenicity, present in more than 90% of patients with idiopathic PD, does not remarkably change in the disease course and is independent from PD motor subtype and severity (2). Marked SN hyperechogenicity is found also 8-13% of adult healthy population and may indicate in them a (subclinical) malfunction of the nigrostriatal dopaminergic system (2, 12). In subjects at ages between 50 and 70 years without PD SN hyperechogenicity is associated with a 20-fold increased risk of developing PD (16). On the other hand more than 80% of healthy subjects who exhibit this TCS abnormality will never develop PD during their lifetime. SN hyperechogenicity has been reported to be present with variable frequencies in a number of other brain diseases such as major depression, attention deficit hyperactivity disorder, and distinct types of dystonia and spinocerebellar atrophy (17). Therefore the application of the TCS finding of SN hyperechogenicity is currently recommended preferably in combination with other markers to assess the potential of developing PD in subjects at risk such as those with idiopathic rapid eye movement sleep behavior disorder (18, 19).

TCS of SN alone is helpful for the discrimination of PD from essential tremor (20-22). For the differentiation of PD from atypical parkinsonian syndromes TCS of SN should be combined with TCS of lenticular nucleus (LN) and third ventricle (**Table 1**) (2, 15, 23-29). The combined presence of normal SN echogenicity and LN hyperechogenicity discriminates atypical parkinsonian syndromes from idiopathic PD with high predictive value (23, 24, 26, 27). In turn, the triad of SN hyperechogenicity, hyposmia and asymmetric motor signs is highly predictive for PD and can be detected already at very early disease stages (30).

The European Academy of Neurology (EAN) and the European Section of the Movement Disorder Society (MDS-ES) recommend TCS for: (I) the differential diagnosis of PD from

atypical parkinsonian syndromes and secondary parkinsonian syndromes, (II) the early diagnosis of PD and (III) the detection of subjects at risk for PD (6).

Table 1 TCS findings in normal population and in patients with various movement disorders (adapted from (15)). Abnormal TCS findings present at least unilaterally in a given individual. The symbols indicate the respective frequency of abnormal findings in the author's lab: -, found in no case; (+), rarely found (<10%); +, occasionally found (10-20%); ++, frequently found (30-50%); +++, very frequently found (>80%).

Syndrome	Hyperechogenic Substantia nigra	Hyperechogenic Lenticular nucleus	3rd Ventricle Width >10mm	Comment
Normal (Age > 50y)	(+)	+	(+)	
Parkinson's disease	+++	+	(+)	
Essential tremor	+	+	(+)	
Multiple-system atrophy	(+)	+++	+	
Richardson syndrome	++	+++	+++	
Corticobasal degeneration	+++ 1	+++	-	1 Bilateral-symmetric
Dementia with Lewy bodies	+++ 1	++	+	1 Bilateral-symmetric
Wilson's disease	++	+++	+	
Idiopathic dystonia	(+)	+++	(+)	

Huntington's disease	++	++ 2	+	2 Hyperechogenic caudate and/or lenticular nuclei

Midbrain raphe should be assessed on TCS only if the basal cisterns and the nucleus ruber are clearly visualized. According to current consensus guidelines only the discrimination of two grades of echogenicity (normal vs reduced) is recommended [Figures 6, 7] (1). Raphe echogenicity should only be classified as reduced if transtemporal investigation from both sides shows a reduced echogenicity, provided adequate imaging conditions.

Remember 4 Midbrain raphe is assessable if basal cisterns, aqueduct and ipsilateral nucleus ruber are clearly displayed.

Figure 7 Grading of midbrain raphe echogenicity. A) TCS image of normal raphe echogenicity (arrow). B) TCS image of moderately reduced raphe echogenicity (arrow). C) TCS image of markedly reduced raphe echogenicity (arrow; no visible raphe echo).

A reduced echogenicity of midbrain raphe has been detected in about 10% of normal population but in 50-70% of patients with depressive disorders (31, 32). The development over time and the morphological substrate of this TCS finding are still unclear, however, it is likely to reflect an alteration of the central serotonergic system (33, 34). Reduced midbrain

raphe echogenicity has been related to suicidal ideation in depressed subjects (35). This TCS finding is also frequent in PD or Huntington's disease patients with associated depression (36-38).

Thalamus plane

The thalamus plane (basal ganglia plane) is approached, if starting from the axial midbrain plane, by tilting the transducer by about 20° in upwards direction [Figure 4]. Even if the bone window is poor the pineal gland mostly is visible due to its calcification which therefore represents an important landmark structure in the basal ganglia plane. The 3rd ventricle appears as a highly echogenic double line between the thalami indicating its lateral borders. Near to the midline in a more frontal position the frontal horns of lateral ventricles are displayed; sometimes it is necessary to tilt the imaging sector somewhat in frontal direction for visualization of frontal horns.

Remember 5 Thalamus plane is adequately displayed if pineal gland, bilateral thalami 3rd ventricle and contralateral frontal horn are clearly visible.

At this plane the widths of 3rd ventricle and contralateral frontal horn are measured. Most authors measure the minimum width of 3rd ventricle (1). The width of contralateral frontal horn is measured, as a standard in the author's lab, at the most frontal position at which the bilateral frontal horns are in junction. Normal ranges of ventricle widths are age-dependent. In subjects under/over the age of 60 widths of >7/>10 mm (3rd ventricle) and >17/>20 mm (frontal horn) are regarded as abnormal (1). Dilatation of 3rd ventricle is a characteristic finding already in early stages of progressive supranuclear palsy (Richardson syndrome), especially if combined with hyperechogenicity of LN (25, 27). Pronounced dilatation of all ventricles points indicates advanced brain atrophy, or hydrocephalus.

Basal ganglia (LN, caudate nucleus) are usually assessed contralaterally to the side of insonation (unlike SN) since the contralateral structures are displayed in larger area in the sector-shape sonogram. Normally these basal ganglia are not discriminable by their echogenicity from the surrounding white matter [Figure 4]. A visually increased echogenicity

of basal ganglia compared to the surrounding white matter is regarded as abnormal finding ("hyperechogenicity") [Figure 8].

Figure 8 **TCS findings of basal ganglia at thalamus level. C = caudate head, F = frontal horn of lateral ventricle, I = insula, L = lenticular nucleus, P = pineal gland, Pl = choroid plexus of dorsal horn of lateral ventricle, T = thalamus. A) Normal basal ganglia TCS. Lenticular and caudate nucleus are indistinguishable from surrounding brain parenchyma. B) Hyperechogenicity of lenticular nucleus (arrow), characteristic for atypical parkinsonian syndromes. C) Markedly hyperechoic, dot-like lesion of lenticular nucleus (arrow) caused by focal calcification as is indicated by high echogenicity similar to that of pineal gland. This finding is usually of no diagnostic relevance. D) Hyperechogenicity of caudate nucleus (arrow), frequently found in Huntington's disease.**

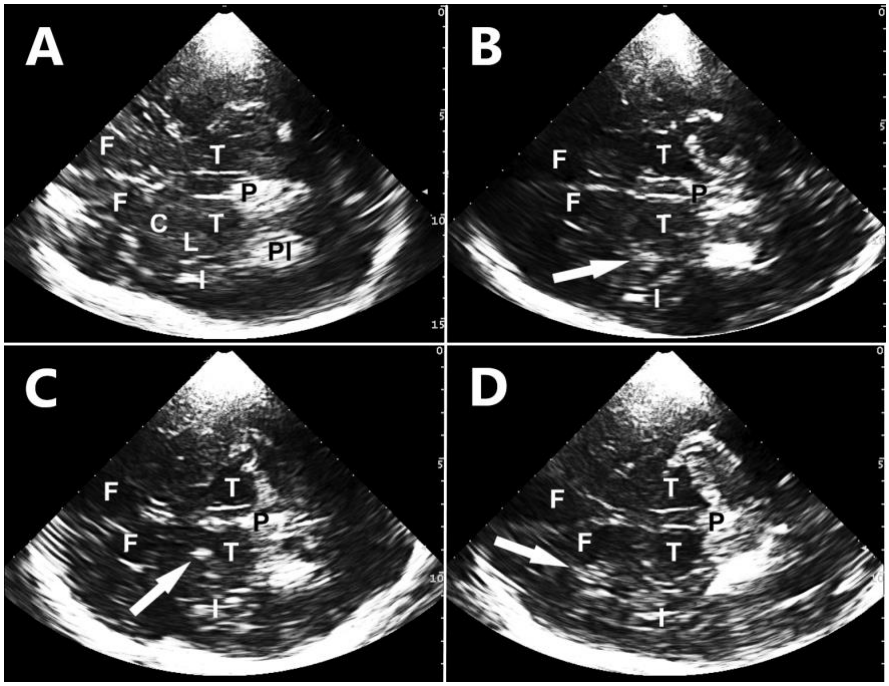

Hyperechogenicity of LN or caudate nucleus usually appears in a circumscribed area rather than as a diffuse change of the referring nucleus. Areas of hyperechogenic basal ganglia lesions may optionally be quantified by planimetric measurements, similar to measurements of SN

hyperechogenicity (39). In this case a hyperechogenicity should only be regarded present at hyperechogenic area >0.20 cm². Other structures can sometimes cause misdiagnosis of a basal-ganglia hyperechogenicity mainly due to their lateral imaging artefacts (e.g. echogenic ventricle borders, basal cisterns). Moreover, especially in patients with very good bone windows reverberation artefacts originating from the highly echogenic ventricular structures (borders, choroid plexus) may mimic basal ganglia hyperechogenicity. To avoid such misdiagnosis the anatomical relationship between the basal ganglia and neighboring structures should be explored by slightly tilting and twisting the transducer (15). LN hyperechogenicity is a frequent albeit not specific finding in patients with generalized, segmental, focal and task-related forms of idiopathic dystonia (15, 39). It is also typically detected in brain disorders with accumulation of iron, manganese, or copper, e.g. in Wilson's disease (40). LN hyperechogenicity supports the discrimination of atypical parkinsonian syndromes from PD (23, 24, 26, 27). Hyperechogenicity of caudate nucleus has been reported as a frequent finding in patients with Huntington's disease (37, 41), which may support the discrimination from other chorea disorders. A pronounced hyperechogenicity of basal ganglia, with brightness similar to that of pineal gland and calcified structures of the chorioid plexus in the dorsal horn of lateral ventricle, indicates calcification and may be found as dot-like lesion in elderly subjects but is more extended in Fahr's disease (2, 42).

Deep brain stimulation electrodes

DBS electrodes are clearly visible on TCS due to their high echogenicity and typical imaging artefacts [Figure 5]. Because of somewhat higher image resolution in the focal zone of the TCS transducer we prefer assessment of DBS electrode position in the basal ganglia ipsilateral to the side of insonation (7). Gross dislocation of a DBS electrode can reliably be detected with TCS. Detailed criteria of optimum and suboptimum DBS electrode location have been reported for DBS of ventro-intermediate thalamic nucleus, globus pallidus interna, and subthalamic nucleus (43). Especially, post-operative control of DBS electrode location in the subthalamic nucleus can easily be executed with TCS [Figure 5].

TCS in neuro-intensive care medicine

While CT and MRI today represent the gold standard in the diagnosis of intracranial hemorrhage, TCS can well be used for the bedside monitoring for the size and resorption of hematomas, and, especially for the monitoring of midline shift and ventricle widths (3). In the acute phase, intracerebral hemorrhage appears homogenous, sharply demarcated and hyperechogenic [Figure 9] (44, 45). The sonographic appearance of intracerebral hemorrhage changes over time with a decrease in echo intensity beginning at the center of the lesion (45). Sonographic 3D volumetry of the hematoma supports outcome prediction (46). The diagnosis of parenchymal bleeding on TCS is however limited in small (<1×1 cm) and cortically located lesions (45). TCS can detect subdural hematoma, and may especially be useful for monitoring the size of subdural hematoma provided sufficient insonability (47). Also, the widths of third and lateral ventricles (frontal horns) can be monitored with TCS, e.g. in patients with intraventricular hemorrhage (48). TCS can well be used for monitoring of midline shift of third ventricle in patients with space-occupying stroke (49). For this, the distance from the TCS probe to the center of third ventricle is measured both from the symptomatic (a) and asymptomatic (b) sides, and the midline shift of third ventricle is then calculated using the formula (a-b)/2 [Figure 9]. It has been shown that TCS monitoring of midline shift is of prognostic value in patients with space-occupying supratentorial ischemic stroke (49). TCS can therefore be regarded as a reliable tool for monitoring the midline shift as well as the ventricular width in patients with acute supratentorial brain lesions who have adequate acoustic bone windows (> 80% of patients).

Figure 9 **TCS assessment of midline shift in a patient with large intracerebral hematoma. A) Distance measure (a = 90 mm) between the transducer face and the compressed third ventricle, with visualization of the acute hemispheric hematoma (triangles) ipsilateral to insonation. B) Distance measure (b = 69 mm) between the transducer face and the compressed third ventricle, with visualization of the acute hemispheric hematoma (triangles) contralateral to**

insonation. The midline shift at the level of third ventricle is calculated as follows: (a-b)/2 (here: 10 mm).

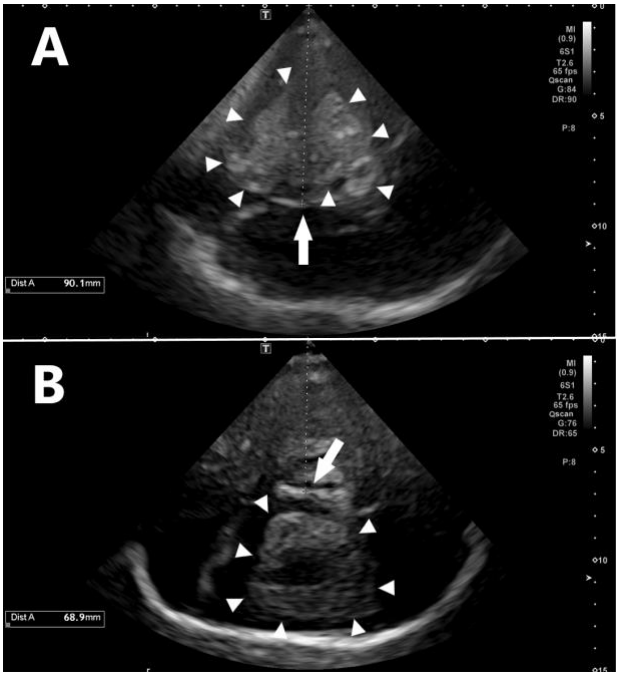

References

1. Walter U, Behnke S, Eyding J, Niehaus L, Postert T, Seidel G, Berg D. Transcranial brain parenchyma sonography in movement disorders: state of the art. Ultrasound Med Biol 2007;33:15-25.
2. Berg D, Godau J, Walter U. Transcranial sonography in movement disorders. Lancet Neurol 2008;7:1044-1055.
3. Harrer JU, Eyding J, Ritter M, Schminke U, Schulte-Altedorneburg G, Köhrmann M, Nedelmann M, et al. The potential of neurosonography in neurological emergency and intensive care medicine: monitoring of increased intracranial pressure, brain death diagnostics, and cerebral autoregulation– part 2. Ultraschall Med 2012;33:320-331; quiz 332-326.
4. Go CL, Frenzel A, Rosales RL, Lee LV, Benecke R, Dressler D, Walter U. Assessment of substantia nigra echogenicity in German and Filipino populations using a portable ultrasound system. J Ultrasound Med 2012;31:191-196.
5. Walter U, Kanowski M, Kaufmann J, Grossmann A, Benecke R, Niehaus L. Contemporary ultrasound systems allow high-resolution transcranial imaging of small echogenic deep intracranial structures similarly as MRI: a phantom study. Neuroimage 2008;40:551-558.

6. Berardelli A, Wenning GK, Antonini A, Berg D, Bloem BR, Bonifati V, Brooks D, et al. EFNS/MDS-ES/ENS [corrected] recommendations for the diagnosis of Parkinson's disease. Eur J Neurol 2013;20:16-34.
7. Walter U, Kirsch M, Wittstock M, Müller JU, Benecke R, Wolters A. Transcranial sonographic localization of deep brain stimulation electrodes is safe, reliable and predicts clinical outcome. Ultrasound Med Biol 2011;37:1382-1391.
8. Walter U. How to measure substantia nigra hyperechogenicity in Parkinson disease: detailed guide with video. J Ultrasound Med 2013;32:1837-1843.
9. van de Loo S, Walter U, Behnke S, Hagenah J, Lorenz M, Sitzer M, Hilker R, et al. Reproducibility and diagnostic accuracy of substantia nigra sonography for the diagnosis of Parkinson's disease. J Neurol Neurosurg Psychiatry 2010;81:1087-1092.
10. Berg D, Godau J, Riederer P, Gerlach M, Arzberger T. Microglia activation is related to substantia nigra echogenicity. J Neural Transm (Vienna) 2010;117:1287-1292.
11. Behnke S, Double KL, Duma S, Broe GA, Guenther V, Becker G, Halliday GM. Substantia nigra echomorphology in the healthy very old: Correlation with motor slowing. Neuroimage 2007;34:1054-1059.
12. Berg D, Becker G, Zeiler B, Tucha O, Hofmann E, Preier M, Benz P, et al. Vulnerability of the nigrostriatal system as detected by transcranial ultrasound. Neurology 1999;53:1026-1031.
13. Hagenah J, König IR, Sperner J, Wessel L, Seidel G, Condefer K, Saunders-Pullman R, et al. Life-long increase of substantia nigra hyperechogenicity in transcranial sonography. Neuroimage 2010;51:28-32.
14. Mehnert S, Reuter I, Schepp K, Maaser P, Stolz E, Kaps M. Transcranial sonography for diagnosis of Parkinson's disease. BMC Neurology 2010;10:9.
15. Walter U, Školoudík D. Transcranial sonography (TCS) of brain parenchyma in movement disorders: quality standards, diagnostic applications and novel technologies. Ultraschall Med 2014;35:322-331.
16. Berg D, Behnke S, Seppi K, Godau J, Lerche S, Mahlknecht P, Liepelt-Scarfone I, et al. Enlarged hyperechogenic substantia nigra as a risk marker for Parkinson's disease. Mov Disord 2013;28:216-219.
17. Walter U. Substantia nigra hyperechogenicity is a risk marker of Parkinson's disease: no. J Neural Transm (Vienna) 2011;118:607-612.
18. Heinzel S, Kasten M, Behnke S, Vollstedt EJ, Klein C, Hagenah J, Pausch C, et al. Age- and sex-related heterogeneity in prodromal Parkinson's disease. Mov Disord 2018;33:1025-1027.
19. Pilotto A, Heinzel S, Suenkel U, Lerche S, Brockmann K, Roeben B, Schaeffer E, et al. Application of the movement disorder society prodromal Parkinson's disease research criteria in 2 independent prospective cohorts. Mov Disord 2017;32:1025-1034.
20. Doepp F, Plotkin M, Siegel L, Kivi A, Gruber D, Lobsien E, Kupsch A, et al. Brain parenchyma sonography and 123I-FP-CIT SPECT in Parkinson's disease and essential tremor. Mov Disord 2008;23:405-410.
21. Heim B, Peball M, Hammermeister J, Djamshidian A, Krismer F, Seppi K. Differentiating Parkinson's Disease from Essential Tremor Using Transcranial Sonography: A Systematic Review and Meta-Analysis. J Parkinsons Dis 2022;12:1115-1123.
22. Stockner H, Sojer M, K KS, Mueller J, Wenning GK, Schmidauer C, Poewe W. Midbrain sonography in patients with essential tremor. Mov Disord 2007;22:414-417.

23. Alonso-Canovas A, Tembl Ferrairó JI, Martínez-Torres I, Lopez-Sendon Moreno JL, Parees-Moreno I, Monreal-Laguillo E, Pérez-Torre P, et al. Transcranial sonography in atypical parkinsonism: How reliable is it in real clinical practice? A multicentre comprehensive study. Parkinsonism Relat Disord 2019;68:40-45.
24. Behnke S, Berg D, Naumann M, Becker G. Differentiation of Parkinson's disease and atypical parkinsonian syndromes by transcranial ultrasound. J Neurol Neurosurg Psychiatry 2005;76:423-425.
25. Ebentheuer J, Canelo M, Trautmann E, Trenkwalder C. Substantia nigra echogenicity in progressive supranuclear palsy. Mov Disord 2010;25:773-777.
26. Monaco D, Berg D, Thomas A, Di Stefano V, Barbone F, Vitale M, Ferrante C, et al. The predictive power of transcranial sonography in movement disorders: a longitudinal cohort study. Neurol Sci 2018;39:1887-1894.
27. Walter U, Dressler D, Probst T, Wolters A, Abu-Mugheisib M, Wittstock M, Benecke R. Transcranial brain sonography findings in discriminating between parkinsonism and idiopathic Parkinson disease. Arch Neurol 2007;64:1635-1640.
28. Walter U, Dressler D, Wolters A, Probst T, Grossmann A, Benecke R. Sonographic discrimination of corticobasal degeneration vs progressive supranuclear palsy. Neurology 2004;63:504-509.
29. Walter U, Dressler D, Wolters A, Wittstock M, Greim B, Benecke R. Sonographic discrimination of dementia with Lewy bodies and Parkinson's disease with dementia. J Neurol 2006;253:448-454.
30. Busse K, Heilmann R, Kleinschmidt S, Abu-Mugheisib M, Höppner J, Wunderlich C, Gemende I, et al. Value of combined midbrain sonography, olfactory and motor function assessment in the differential diagnosis of early Parkinson's disease. J Neurol Neurosurg Psychiatry 2012;83:441-447.
31. Becker G, Becker T, Struck M, Lindner A, Burzer K, Retz W, Bogdahn U, et al. Reduced echogenicity of brainstem raphe specific to unipolar depression: a transcranial color-coded real-time sonography study. Biol Psychiatry 1995;38:180-184.
32. Krogias C, Walter U. Transcranial Sonography Findings in Depression in Association With Psychiatric and Neurologic Diseases: A Review. J Neuroimaging 2016;26:257-263.
33. Becker G, Berg D, Lesch KP, Becker T. Basal limbic system alteration in major depression: a hypothesis supported by transcranial sonography and MRI findings. Int J Neuropsychopharmacol 2001;4:21-31.
34. Kostić M, Munjiza A, Pesic D, Peljto A, Novakovic I, Dobricic V, Tosevski DL, et al. A pilot study on predictors of brainstem raphe abnormality in patients with major depressive disorder. J Affect Disord 2017;209:66-70.
35. Budisic M, Karlovic D, Trkanjec Z, Lovrencic-Huzjan A, Vukovic V, Bosnjak J, Demarin V. Brainstem raphe lesion in patients with major depressive disorder and in patients with suicidal ideation recorded on transcranial sonography. Eur Arch Psychiatry Clin Neurosci 2010;260:203-208.
36. Berg D, Supprian T, Hofmann E, Zeiler B, Jäger A, Lange KW, Reiners K, et al. Depression in Parkinson's disease: brainstem midline alteration on transcranial sonography and magnetic resonance imaging. J Neurol 1999;246:1186-1193.
37. Krogias C, Eyding J, Postert T. Transcranial sonography in Huntington's disease. Int Rev Neurobiol 2010;90:237-257.

38. Walter U, Hoeppner J, Prudente-Morrissey L, Horowski S, Herpertz SC, Benecke R. Parkinson's disease-like midbrain sonography abnormalities are frequent in depressive disorders. Brain 2007;130:1799-1807.
39. Naumann M, Becker G, Toyka KV, Supprian T, Reiners K. Lenticular nucleus lesion in idiopathic dystonia detected by transcranial sonography. Neurology 1996;47:1284-1290.
40. Walter U. Transcranial sonography in brain disorders with trace metal accumulation. Int Rev Neurobiol 2010;90:166-178.
41. Kozel J, Školoudík D, Ressner P, Michalčová P, Dušek P, Hanzlíková P, Dvořáčková N, et al. Echogenicity of Brain Structures in Huntington's Disease Patients Evaluated by Transcranial Sonography - Magnetic Resonance Fusion Imaging using Virtual Navigator and Digital Image Analysis. Ultraschall Med 2023.
42. Brüggemann N, Schneider SA, Sander T, Klein C, Hagenah J. Distinct basal ganglia hyperechogenicity in idiopathic basal ganglia calcification. Mov Disord 2010;25:2661-2664.
43. Walter U, Müller JU, Rösche J, Kirsch M, Grossmann A, Benecke R, Wittstock M, et al. Magnetic resonance-transcranial ultrasound fusion imaging: A novel tool for brain electrode location. Mov Disord 2016;31:302-309.
44. Mäurer M, Shambal S, Berg D, Woydt M, Hofmann E, Georgiadis D, Lindner A, et al. Differentiation between intracerebral hemorrhage and ischemic stroke by transcranial color-coded duplex-sonography. Stroke 1998;29:2563-2567.
45. Seidel G, Kaps M, Dorndorf W. Transcranial color-coded duplex sonography of intracerebral hematomas in adults. Stroke 1993;24:1519-1527.
46. Niesen WD, Schlaeger A, Bardutzky J, Fuhrer H. Correct Outcome Prognostication via Sonographic Volumetry in Supratentorial Intracerebral Hemorrhage. Front Neurol 2019;10:492.
47. Niesen WD, Burkhardt D, Hoeltje J, Rosenkranz M, Weiller C, Sliwka U. Transcranial grey-scale sonography of subdural haematoma in adults. Ultraschall Med 2006;27:251-255.
48. Kiphuth IC, Huttner HB, Struffert T, Schwab S, Köhrmann M. Sonographic monitoring of ventricle enlargement in posthemorrhagic hydrocephalus. Neurology 2011;76:858-862.
49. Gerriets T, Stolz E, Modrau B, Fiss I, Seidel G, Kaps M. Sonographic monitoring of midline shift in hemispheric infarctions. Neurology 1999;52:45-49.